Biofuels and Environmental Biotechnology **Biotechnology and Bioengineering**
DOI 10.1002/bit.26332

Quantitative proteome profiles help reveal efficient xylose utilization mechanisms in solventogenic Clostridium sp. strain BOH3†

Anindya Basu[1,4], Fengxue Xin[1], Teck Kwang Lim[2], Qingsong Lin[2], Kun-Lin Yang[3], Jianzhong He[1]*

[1] Department of Civil and Environmental Engineering, National University of Singapore, Republic of Singapore

[2] Department of Biological Sciences, National University of Singapore, 14 Science Drive 4, Singapore 117543

[3] Department of Chemical and Biomolecular Engineering, National University of Singapore.

[4]School of Pharmaceutical Sciences, Rajiv Gandhi Technical University, Bhopal, M.P., India

*** Corresponding author:**

Department of Civil and Environmental Engineering National University of Singapore Block E2-02-13 1 Engineering Drive 3, Singapore 117576

Phone: (65) 6516-3385;

Fax: (65) 6779 1635

Email: jianzhong.he@nus.edu.sg

†This article has been accepted for publication and undergone full peer review but has not been through the copyediting, typesetting, pagination and proofreading process, which may lead to differences between this version and the Version of Record. Please cite this article as doi: [10.1002/bit.26332]

Additional Supporting Information may be found in the online version of this article.

Received February 20, 2017; Revision Received April 13, 2017; Accepted May 1, 2017

Abstract

Development of sustainable biobutanol production platforms from lignocellulosic materials is impeded by inefficient five carbon sugar uptake by solventogenic bacteria. The recently isolated *Clostridium* sp. strain BOH3 is particularly advantaged in this regard as it serves as a model organism which can simultaneously utilize both glucose and xylose for high butanol (>15 g/L) production. Strain BOH3 was therefore investigated for its metabolic mechanisms for efficient five carbon sugar uptake using a quantitative proteomics based approach. The proteomics data show that proteins within the *CAC1341-1349* operon play a pivotal role for efficient xylose uptake within the cells to produce butanol. Furthermore, up-regulation of key enzymes within the riboflavin synthesis pathway explained that xylose could induce higher riboflavin production capability of the bacteria (e.g., ~80 mg/L from glucose vs ~120 mg/L from xylose). Overall results from the present experimental approach indicated that xylose-fed BOH3 cultures are subjected to high levels of redox stress which coupled with the solvent stress - trigger a sporulation response within the cells earlier than the glucose-fed cultures. The study lays the platform for metabolic engineering strategies in designing organisms for efficient butanol and other value-added chemicals such as riboflavin production.

Keywords: iTRAQ; proteome dynamics; biofuels; *Clostridium*, BOH3

Introduction

Efforts to cope-up with the fluctuating fuel prices, while simultaneously addressing the ecological stress induced by petrochemical based products, has raised the need for microbial based methods to convert lignocellulosic waste materials into biofuels (Jones et al. 2015; Zheng et al. 2009). A huge amount of lignocellulosic materials are discarded by every walk of life, which can be used for harnessing significant amounts of energy (Kim and Dale 2015; Peralta-Yahya et al. 2012). Bioconversion of these materials through anaerobic fermentative strategies, particularly using solventogenic *Clostridium* strains, has been proposed to be a promising option to establish sustainable energy production platforms (Bankar et al. 2013; Peralta-Yahya et al. 2012). However, lignocellulose (being made up of five and six carbon sugars) consumption is impeded by the ineffective five-carbon uptake by solventogenic *Clostridium* strains (Zaldivar et al. 2001). In fact, the inefficient five carbon utilization seems to be a major obstacle, overcoming which can help resolve the bottlenecks currently impeding establishment of sustainable biobutanol production platforms. Consequently, several attempts have been made recently on the commercial bacteria - *C. acetobutylicum* strain ATCC824 to better understand its incapability to uptake five-carbon sugars like xylose so as to identify metabolic engineering strategies to improve xylose utilization (Grimmler et al. 2010; Haus et al. 2011; Janssen et al. 2010; Sivagnanam et al. 2011). However, majority of the attempts to metabolically engineer strain ATCC824 did not end up with mutants exhibiting similar solvent producing characteristics as the glucose-fed parent organism (Hu et al. 2011; Jin et al. 2014; Li et al. 2012).

In contrast to the widely used strain ATCC824, a novel wild-type *Clostridium* sp. strain BOH3, capable of simultaneously utilizing both five and six carbon sugars was recently discovered (Bramono et al. 2011; Xin et al. 2014) by our group, thereby providing a quantum

leap towards establishing sustainable strategies for bioconversion of lignocellulosic materials into butanol. This strain thus provides an ideal platform for studying the metabolic machineries that needs to be in-place within a solventogenic *Clostridium* to ensure successful utilization of five-carbon sugars like xylose. Strain BOH3 was also found to exhibit unique fermentation characteristics considering the fact that in contrast to glucose-fed cultures, the xylose-fed cells were able to produce equivalent titres (slightly higher) of butanol along with significantly higher yields of riboflavin, another commercially relevant chemical. Obtaining such valuable by-products actually help in improving commercial feasibility of the bioprocessing platform and provide impetus to dig deeper into the bacterial metabolic machineries to understand the differences between the glucose and xylose utilization pathways.

In this study an iTRAQ^{TM} (isobaric tag for relative and absolute quantitation) based proteomics strategy (Ghosh et al. 2013; Ghosh et al. 2011; Ross et al. 2004) was applied to the bacterial samples at different fermentation stages to identify key proteins involved and the cellular responses to high xylose utilization. Particularly, efforts were directed towards identifying pathways that help in effortless xylose utilization by the bacteria, while simultaneously produce riboflavin.

Materials and Methods

Bacteria culture and sampling

Strain BOH3 was grown in 160 mL serum bottles consisting of 50 mL mineral salts medium as described previously (Bramono et al. 2011; He et al. 2003; Xin et al. 2014), unless stated otherwise. The cells were grown in duplicates, as biological replicates, either in presence of 60 g/L glucose or xylose as the carbon source under anaerobic conditions in a shaking incubator (135 rpm) at 35°C. After 24 h of fermentation, the bacterial cultures were maintained at pH = 5.0 by dosing with 2 M NaOH solution. For the proteomics analysis, 25

mL cultures were collected from the serum bottles at two different time-points: first after about 24 h of incubation, i.e., during the late acidogenesis phase of the bacterial growth cycle and the second after about 48 h of incubation, i.e., at the mid-solventogenesis phase of the culture (Fig. S1). Following sample collection, the cells were washed with PBS (phosphate buffered saline) buffer for at least three times to remove the extracellular proteases (Hou et al. 2013) and stored at -80°C freezer until further usage. Protein was extracted from all cell pellets within two days of harvesting. The corresponding phases of the fermentation cultures were verified through measurement of concentrations of the produced volatile fatty acids and solvents using GC-FID as described later. For the sake of convenience, biological replicate samples collected at the acid phase are termed as APG1/2 and APX1/2 for the cells growing in presence of glucose and xylose, respectively (Fig. 1A). Similarly, the samples collected during the solvent phase are termed as SPG1/2 and SPX1/2, for the cells growing in presence of glucose and xylose, respectively (Fig. 1A).

Protein extraction and iTRAQ sample preparation

Methodology adopted for protein extraction from different bacterial samples was optimized based on the findings of Hou *et al*. (Hou et al. 2013). Cell pellets collected were re-suspended in 2 mL of an optimized lysis buffer consisting of 4% CHAPS, 0.5 M TEAB, 1% $CaCO_3$ and subjected to sonication for 5 min (pulses used: 7 sec on and 5 sec off). The obtained cell debris were separated by centrifugation (12000 x *g* for 15 min) at 4 ºC and the supernatant protein concentrations were measured using the RCDC Protein Quantification kit (Bio-Rad, Singapore), according to the manufacturer's protocol.

iTRAQ labelling was carried out using the iTRAQ Reagent 8-Plex kit (AB Sciex, Singapore) according to manufacturer's protocol with minor modifications. The biological replicates APG1 and APG2 were labelled with iTRAQ labelling reagents 113 and 114; while the replicates APX1 and APX2 were labelled with reagents 115 and 116. Samples collected

at the solvent phase SPG1 and SPG2 were labelled with reagents 117 and 118 respectively; while samples SPX1 and SPX2 were labelled with reagents 121 and 119, respectively. The iTRAQ workflow used within the current study is presented in Figure 1A. Briefly, the protein samples were first reduced with tris-(2-carboxyethyl) phosphine (TCEP) followed by cysteine blocking (alkylation) with methyl methane-thiosulfonate (MMTS). The samples were then diluted 20 times and digested into peptides by incubating them in trypsin (w/$CaCl_2$; Promega) at 37 ºC for 16 h with an enzyme to protein ratio of 1:10 (w/w). The digested peptides were then dried and reconstituted with 0.5 M TEAB and were then labelled with the respective isobaric tags through incubation at room temperature for 2 h before combining them together.

Interfering substances including excess reducing agent (TCEP), alkylating agent (MMTS), SDS, calcium chloride, excess iTRAQ reagents etc., were removed through strong cation exchange chromatography of the pooled samples, as provided in the iTRAQ Method Development Kit (AB SCIEX). The eluted fraction was desalted using Sep-Pak C18 cartridges (WATERS), dried and then reconstituted in 20 mM Ammonium formate buffer-pH 10 for 2D LC- MS/MS analysis and subsequent data analysis as detailed in Supplementary notes. The obtained mass spectrometry proteomics data have been deposited to the ProteomeXchange Consortium via the PRIDE (Vizcaíno et al. 2016) partner repository with the dataset identifier PXD005239. Strategies adopted for the LC MS/MS data analysis are also detailed in the supplementary notes.

Flow cytometry

Aliquots from the BOH3 samples collected for the proteomics studies were characterised using a BD AccuriC6 flow cytometer (BD Biosciences, Singapore), where the blue laser (λ = 488 nm, 20 mW) was used for conducting the experiments. Forward-scatter characteristics (FSC) and side-scatter characteristics (SSC) were detected as small- and large- angle scatters of the 488-nm laser, respectively. All flow-cytometric analyses were performed by

thresholding on SSC to remove noise. Green fluorescence was detected using a 533/30 nm band-pass filter while red fluorescence was detected by a 670 nm long-pass filter. Bacterial viability and metabolic activity were assayed by staining the cells with the LIVE/DEAD Bacterial viability kit and Bac*Light*^{TM} *RedoxSensor*^{TM} Green vitality kit (Life technologies, Singapore) respectively, as per the manufacturer's protocol with minor modifications.

For the cell viability assay, 1 mL of the cells were pelleted down and washed with 1% NaCl (1 mL). The cells were re-suspended in 200 µL of 1% NaCl and stained with the propidium iodide and Syto9 (Tracy et al. 2008) to stain the dead and live bacterial cells, respectively (Mishra et al. 2014).

For the metabolic activity assay, cell pellets obtained from 1 mL culture were washed with 1 mL PBS and re-suspended in 200 µL of the same buffer, and then 10 µL of the sample was added to 1 mL of PBS to which 2 µL of 10x diluted Redox Sensor Green dye was added and stained in the dark for at least 10 min. The treated bacterial cells were immediately analyzed following the staining procedure.

Bacterial growth and biosolvents analysis

Details provided in supplementary notes.

Results

Glucose and xylose-fed BOH3 cells showed significant differences in culture characteristics

Strain BOH3 was allowed to grow in glucose or xylose as the sole carbon source and the rate of sugar consumption was monitored. Impressively, the glucose and xylose consumption rate was found to be similar, where complete consumption of both the sugar substrates was observed within 60 h of fermentation (Fig. S1) (Xin et al. 2014). Furthermore, though the final butanol amount obtained upon completion of the batch fermentations

remained comparable for both substrates (slightly higher for the xylose-fed cultures), the amount of riboflavin produced by the bacteria from xylose was significantly higher compared to that obtained from glucose (Fig. 2).

To better understand the bacterial response towards xylose and glucose substrates, culture samples were taken at time points corresponding to the late- acidogenic phase and the mid- solventogenic phases of the fermentation (as specified in the materials and methods section and indicated in Fig. S1) and subjected to proteomics analysis as described in latter sections. The bacterial populations used for performing the proteomics experiment were characterized through viability assay and bacterial reductase activity assay using flow-cytometry. The latter assay was performed through staining of the bacteria using a dye which is an indicator of the bacterial membrane reductase activity, thereby enabling to monitor the electron transport chain function within the desired bacterial population (Yeom et al. 2010). Interestingly, despite the similarity in bacterial growth as determined through optical density measurements (Fig. S1), cell populations growing under xylose and glucose showed marked differences, particularly during the solvent phase (Fig. 3). Such differences were however, not significant during the earlier stages of the fermentation. As shown in Figure 3B, cell viability assay indicated the presence of a diversified bacterial population in the xylose-fed culture during the solvent phase where the marked region, representing approximately 26% of the cell population, showed higher green fluorescence in the flow cytometry profile. The remaining bacterial population seemed to exhibit varying levels of green and red fluorescence, indicating that large part of the population were probably in different stages of their life cycle. Aligned to such an observation, Figure 3D also indicated the presence of two distinct populations where approximately 56% of the bacterial cells, showing higher green fluorescence (the marked region in Fig. 3D), could be considered metabolically more active

than the others. Such significant cell population differentiation was not observed for the cells grown with glucose as a substrate, as shown in Figure 3E to H.

iTRAQ labelling strategy and data interpretation revealed different aspects of BOH3 fermentation

The iTRAQ labelling approach was designed to obtain extensive information about the bacterial proteome under different culture growth conditions using a single experiment through proper usage of the achievable iTRAQ ratios (Fig. 1A). For instance, as indicated in Figure 1B, the iTRAQ ratios of 115 : (113 or 114) and 116 : (113 or 114) would indicate protein regulation for xylose-fed cultures against glucose-fed cultures during the acidogenesis phase (for convenience the replicates corresponding to these ratios would be termed as "AP1/2"). Similarly, the proteome changes of the xylose-fed cultures with respect to glucose-fed cultures during the mid-solventogenesis phase can be obtained from the following iTRAQ ratios - 119 : (117 or 118) and 121 : (117 or 118) (For convenience, the replicates corresponding to these ratios would be termed as "SP1/2"). On the other hand, substrate-specific proteome dynamics indicating the changes within the bacterial cells from the acid phase to the solvent phase can be determined through the following ratios- 119:115 and 121:116 for the case of xylose fed cultures (referred to as "Xylose-dynamics" or "Xyl-1/2"). Similarly, the ratios - 117:113 and 118:114 indicate the proteome dynamics that allow the bacterial transition from the acidogenesis phase to the solventogenesis phase when glucose is used as the sole carbon source (referred to as "Glucose-dynamics" or "Gluc-1/2").

The mass spectrometric data as obtained from the iTRAQ-based proteomics experiment were subjected to rigorous analysis to identify the proteins obtained from the detected peptides. A strict cut-off for unused protein score ≥1.3, as the first qualification criteria, corresponding to 95% confidence level and 2% false discovery rate, yielded the detection of a total of 838 proteins out of which 820 proteins could be quantified ,

representing approximately 20% of the entire bacterial proteome. As shown in Figure 4A the identified proteins represented all major functional groups within the Clusters of Orthologous Genes (COG) classification, thereby indicating the possibility to predict the plausible changes within different bacterial metabolic systems. Subsequently to identify up- or down-regulation of proteins, a cut-off value was determined based on the biological replicate method, since biological variations represent the highest variability in protein expression ratios, compared to other replicates (Chee et al. 2007; Ghosh et al. 2013; Ghosh et al. 2011). The protein expression ratio revealed ~ 25% variation corresponding to 88% data coverage for the case of AP1/2 and SP1/2 (Fig. S2A, B). Hence to compare the protein regulations during the acid or the solvent phases, the cut-off value was fixed at 1.25 fold, corresponding to the iTRAQ ratio of >1.25 for up-regulation and <0.8 for down-regulation. Based on this strict cut-off strategy, a total of 224 proteins were found to be regulated within the AP replicates while 176 proteins were regulated in the SP replicates (as shown in Fig. 4B in the form of a heatmap along with the corresponding COG classification, details presented in Table SI). Similarly for the case of Glucose and Xylose proteome-dynamics, approximately 35% variation corresponded to 88% data coverage (Fig. S2C, D), thereby indicating the ratio of >1.35 for up-regulation and <0.74 for down-regulation for both xylose and glucose fermentations. Regulation of the classes of proteins with respect to Xylose- and Glucose-dynamics is presented within the heatmap in Fig. 4B, where only 84 proteins were found to be regulated for cultures fed with xylose as the sole carbon source as opposed to only 38 proteins regulated within the glucose-fed cultures (details presented in Tables SII and SIII, respectively).

To adopt a systematic approach, attention was first focussed on the proteome changes observed at particular phases of the fermentation (i.e., AP and SP) followed by the proteome dynamics involved in the substrate specific phase changes within the fermenting bacteria. Considering that the primary objective of this work is to shed light on the xylose utilization

capability of strain BOH3, in the following sections discussions would be focused on specific classes of proteins regulated *viz.* proteins related to carbohydrate, transcription, energy and coenzyme metabolisms.

Xylose fermentation initiates regulation of several flavoproteins related to energy metabolism

Regulation pattern of the proteins related to energy metabolism (COG-C) is shown in Figure 5, where the regulated proteins could be classified into five distinct clusters: C1 to C5. Groups C1 and C5 represent proteins which remain either up-regulated or down-regulated throughout xylose fermentation, respectively. Group C2, on the other hand, consisted of proteins that showed relative down-regulation during the solvent phase compared to that in the acid phase. Interestingly majority of the proteins belonging to the groups C1 and C2 consisted of proteins that contain either Fe-S clusters or flavin moieties as their prosthetic groups. Proteins within group C3, *viz*. CAC2542-2544, showed down-regulation only in the solvent phase during the xylose fermentation. It is worth mentioning that the candidates within this group, particularly the proteins CAC2543-2544, are electron-transferring flavoproteins and significantly down-regulated during the solvent phase compared to the acid phase. Proteins within group C4 also comprised of flavoproteins or Fe-S containing proteins involved in redox stress response within the bacterial cells. As shown in Figure 5 this group comprised of proteins that showed marked up-regulation during the solvent phase of xylose fermentation; in fact these proteins remained down-regulated during the acid phase but were significantly up-regulated when the cells enter the solvent phase.

Xylose-fed bacterial cells show marked up-regulation of the Riboflavin synthesis pathway

Considering that majority of the up-regulated COG-C proteins were flavoproteins (as discussed in the previous section), which obtain their flavin moieties from riboflavin molecules within the cell (Lehninger et al. 2008), attention was focussed towards proteins

involved in co-enzyme metabolism, i.e., proteins belonging to the COG-H cluster. The regulation profile of a set of selective COG-H proteins, as obtained from iTRAQ data, is shown in Figure 6. Among the different players within this group, the proteins CAC0590-0593 (*viz.*, ribD, ribB, ribA and ribH, respectively) together represent the entire riboflavin biosynthesis pathway (Fig. 6B) and were found to be up-regulated throughout the xylose fermentation phases. It could thus be safely concluded that the xylose metabolism leads to up-regulation of the riboflavin biosynthesis pathway which is further corroborated by the higher yields of riboflavin from the xylose-fed BOH3 cultures (Fig. 2). Apart from catering the flavoproteins, riboflavin molecules are also known to be involved in iron-uptake within the bacteria (Crossley et al. 2007) which was also revealed in the present case (Fig. 6C). Fermentation studies revealed that riboflavin yields were significantly decreased with increasing Fe^{2+} concentrations within the media, thereby indicating that excess riboflavin produced by the xylose-fed BOH3 cells could also be a part of its effort to facilitate iron uptake.

Proteins within the CAC1341-1349 operon play major roles in xylose utilization in strain BOH3

Several putative genes have been proposed to be involved in the uptake and utilization of five carbon sugars including xylose for *C. acetobutylicum* (Grimmler et al. 2010). The experimental design adopted in this study helped to pin-point the proteins involved in each and every step related to efficient xylose utilization by strain BOH3. Several proteins related to carbohydrate metabolism were found to be regulated through the iTRAQ experiment and is presented in Table-SI. Among the diverse proteins affected during xylose metabolism, regulation pattern of some of the important ones is shown in Figure 7A. Of particular interest are proteins CAC1341-CAC1349 and CAC2610-CAC2613, which form two distinct operons

(their corresponding maps are shown in Fig. 7B) and were found to be up-regulated in both phases of the fermentation.

The CAC1341-CAC1349 seems to be particularly important considering that xylose can be absorbed within the bacterial cells using the sugar-proton symporter CAC1345 and is then converted into xylulose (Grimmler et al. 2010; Jin et al. 2014). This conversion is known to be catalyzed by specific isomerases like CAC1342, CAC1346 and CAC2610, all of which were found to be up-regulated within strain BOH3 throughout the acid and solvent phases. Phosphorylation of the obtained xylulose is then carried out by the kinases like CAC1344 and CAC2612. The subsequent conversion of the xylulose phosphate into catabolic intermediates like glyceraldehyde-3 phosphate and fructose-6 phosphate can be achieved through the combined action of a transketolase (CAC1348) and transaldolase (CAC1347). Despite the presence of other homologous proteins within the cell, the two operons (CAC1341-CAC1349 and CAC2610-CAC2613) remained up-regulated for both phases of fermentation, indicating the importance of the involved proteins for efficient xylose utilization. Important to note here that the catabolite control protein A (*ccpA* or CAC3037), known to control catabolite utilization within bacteria did not show signs of regulation during the fermentation stages (Fig. 7), as had been observed in another study (Grimmler et al. 2010).

Apart from demonstrating the xylose degradation capability of the BOH3 cells, xylose metabolism within strain BOH3 also initiated the expression of phospho-transferase systems (PTS) like CAC0233 and CAP0066-CAP0068 involved in uptake of other types of carbohydrates (Table-SI). Furthermore, several enzymes capable of hydrolyzing complex carbohydrates like the xylanase (CAC3017), endoglucanase (CAC2807), beta-xylosidase (xynD) and beta-glucosidases (CAC1405, CAP0010) were also up-regulated within strain BOH3 particularly during the solvent phase, thereby indicating the potential of the bacteria to

utilize other complex lignocellulosic materials for its survival. Such observations indicate that small quantities of xylose can induce production of xylanolytic enzymes which can further help degrading complex carbohydrates like xylan or cellulose, as has been observed in our lab (Bramono et al. 2011).

Xylose fermentation leads to redox stress that may trigger sporulation response

To understand the differences in the observed cell population characteristics (Fig. 3), attention was focused towards the iTRAQ ratios for proteins corresponding to the Glucose and Xylose-dynamics (defined previously) along with the AP / SP ratios. A closer look at Fig. 4B indicated that significantly large number of regulated proteins related to xylose dynamics belong to the clusters of energy metabolism (COG-C) and protein processing / PTM (COG-O). Table-I presents the function and the iTRAQ ratios of the regulated proteins, where several proteins related to redox-stress response were found to be highly up-regulated. Within the COG-C cluster, several Fe-S containing (flavo-) proteins like the Desulfo-ferrodoxin, Flavo-diiron protein and others, strongly related in addressing free radical detoxification pathway within *Clostridia* (Caranto et al. 2014; Hillmann et al. 2009; Riebe et al. 2007), were found to be up-regulated. Such a stress response was also reflected within the up-regulated proteins corresponding to the COG-O cluster where majority of the regulated proteins were found to be related to processing of proteins within metabolically stressed cells. Particularly, up-regulation of proteins like Thioredoxin reductase, Glutathione and thiol peroxidases - known to be potential gene expression regulators under oxidative stress, strongly indicated the development of the redox stress within the cells (Fomenko et al. 2011). The above-mentioned observations, indicated that in contrast to glucose-fed cultures (as shown in Table 1) the BOH3 cells metabolising xylose were subjected to two-fold stress: the external solvent stress and an internal redox stress.

A possible synergistic response due to the above-mentioned stresses was also reflected in the regulated transcription factors (COG-K cluster proteins), as shown in Table-SI and II. For instance, up-regulation of the phage shock protein A (*pspA*) was observed in the xylose-fed BOH3 cells which is the predominant form of the *psp* proteins in response to conditions leading to lowering of proton-motive force (PMF) within the bacteria including solvent stress (Darwin 2005). Usually bacteria express the *pspA* protein so that it can predominantly bind to the bacterial membrane system in an effort to restore the desired PMF. Aligned to the loss of PMF within the bacteria, down-regulation of the *LytR* protein, part of the *LytSR* two-component system, was also observed (Table SII). This system is known to be a membrane-bound transcription factor that monitors the PMF across the bacterial membrane and its down-regulation can lead to *cidABC* and *lrgAB* operons-mediated autolytic response within the cell (Shala et al. 2013).

Apart from the above mentioned proteins, two other transcription factors *viz, GntR* (CAC0599) and *AbrB* (CAC3647) were also found to be regulated in response to the xylose fermentation. The *GntR* family of proteins are known to respond to changing micro-environments and are also known to regulate proteins in their neighbourhood (Hoskisson and Rigali 2009). In the present case, STRING database (Szklarczyk et al. 2011) search for the identified protein CAC0599 revealed the presence of spore germination genes like *GerKABC* in its neighbourhood, indicating bacterial attempts towards modulation of its capacity to germinate any new spores into vegetative forms. The down-regulation of the *GntR* was also associated with simultaneous down-regulation of the *AbrB* gene which is known to be an important component that maintains the vegetative form of the bacteria (Phillips and Strauch 2002; Robertson et al. 1989; Wang et al. 2013). In fact a down-regulation of the *AbrB* gene during xylose fermentation was observed, indicating the plausible initiation of phospho-relay involved in sporulation (Phillips and Strauch 2002; Robertson et al. 1989), which is further

supported by the relative up-regulation of the *disA* protein (within xylose-fed cultures) involved in DNA repair prior to sporulation (Oppenheimer-Shaanan et al. 2011; Römling 2008). These findings indicate the plausible tendency of the xylose-fed cultures to initiate a sporulation response slightly earlier than the glucose-fed cultures.

Discussion

Inefficient xylose utilization by *C. acetobutylicum* ATCC824 is a major bottleneck for sustainable biobutanol production. Some of the previous studies have demonstrated improved xylose utilization in *Clostridium* through the addition of extracellular electron shuttles like the hydroquinone reducing equivalents (Ye et al. 2011; Ye et al. 2013). Strain BOH3 however, was particularly interesting in this regard since it could show complete xylose utilization under normal fermentation conditions. Other researchers in this field have largely taken the *ccpA* (CAC3037) gene accountable for the inefficient xylose utilization owing to its associated over-expression upon exposure to five carbon sugars - leading to catabolite repression (Grimmler et al. 2010; Ren et al. 2010; Ren et al. 2012). In fact significant improvement in xylose uptake was recently achieved in mutants possessing deleted or disrupted form of this gene (Ren et al. 2010). However, in the present study the proteomic analysis on strain BOH3 indicated no significant changes in the expression of the *ccpA* protein between cells fed with either glucose or xylose (Fig. 7A). Hence, it can be considered that compared to the *ccpA* gene present in other solventogenic *Clostridium*, this particular gene in strain BOH3 remains repressed. Consequently the operon CAC1341-CAC1349, which is under the negative control of the *ccpA* protein and contains a xylose symporter (CAC1345), remains up-regulated throughout the xylose fermentation, thus explaining the capability of the bacteria to utilize five-carbon sugars. Such observation is contrary to that obtained from strain ATCC824, where xylose exposure is known to induce repression of the above operon (Grimmler et al. 2010). Recent studies on the *ccpA* protein,

however, has revealed that it possesses pleiotropic functions, capable of impacting the global cellular metabolic functions in strain ATCC824 (Li et al. 2012; Ren et al. 2010; Ren et al. 2012). It is thus plausible that the distinctive behaviour of the xylose fed BOH3 cultures (Fig. 2 and 3), could be a consequence of its *ccpA* expression profile.

Considering the significant roles played by the *ccpA* protein in *Clostridium* species (Ren et al. 2012), it is highly probable that it helps to maintain a balance in the metabolic flow within the bacteria. Hence with the apparent repression of the protein in strain BOH3, it seems that the bacteria starts losing its control over the carbohydrate metabolism, as can be seen through the modulation of the *LytR* protein (Table SII), indicating an overflow metabolism within the cell (Sadykov and Bayles 2012). The *Clostridium* metabolism, on the other hand, being rich in iron containing proteins (Vasileva et al. 2012) leads to increased demands of Fe. Hence upon restricting the amount of iron within the medium, the cells start producing excess riboflavin (an electron donor) in an attempt to reduce any available Fe^{3+} ions into the easily absorbable Fe^{2+} form (Crossley et al. 2007). This hypothesis is further supported by the significantly lowered riboflavin productivities with increasing Fe^{2+} concentration within the fermentation medium (Fig. 6C), indicating a reduction in riboflavin demands associated with Fe^{2+} abundance. Interestingly the ferric uptake regulator (*Fur*, CAC1682) protein (Helmann 2014), which controls iron absorption within the cells, did not show any signs of regulation in the proteomics dataset, further supporting an unhindered iron-uptake by the cells. However, efficient Fe^{2+} ion utilization within the bacterial cells depends on a delicate metabolic balance, where on the one hand the ions are essential for production of vital enzymes while on the other hand due to its oxidizing tendency, Fe^{2+} tends to induce free radical generation in the bacterial cells, thereby destabilizing the cellular proteins including the Fe-S cluster containing proteins (Cornelis et al. 2011; Vasileva et al. 2012). As a consequence, several proteins related to redox stress response within the cell were found to

be regulated in the xylose-fed BOH3 cultures, particularly during the solvent phase (Fig. 4B and Table SII). The apparent change of the redox potential of the xylose-fed BOH3 is also evident from the regulation of transcription factors like the *LytR* and *pspA*, both of which are induced upon changes in the cellular proton motive force, the latter being also induced in presence of solvent stress like ethanol (Darwin 2005; Model et al. 1997; Sadykov and Bayles 2012). Hence it could be concluded that though the butanol amount achieved through glucose or xylose remains more or less the same, but for the latter case the bacteria remain exposed to high levels of oxidative stress. The combined stress response seems devastating enough for the bacteria to trigger a sporulation response as evidenced by the down-regulation of the *abrB* protein (Phillips and Strauch 2002; Robertson et al. 1989). In fact as shown in Figure 3, the xylose fed cultures seem to remain under different metabolic states which is also reflected by the down-regulation of electron-transport proteins during the solvent phase (Fig. 5, group C3).

Hence to summarize the overall findings of the current work (Fig. 8), strain BOH3 is highly capable of uptaking xylose and regulating metabolism related proteins when exposed to the five carbon sugar, owing to the apparent repression of the inhibitory *ccpA* protein. Such a metabolic setup helps to efficiently utilize xylose, on the other hand, it leads to increased iron demands, leading to higher riboflavin production under Fe^{2+} restricted conditions. Such metabolic consequences can ultimately result in increased cellular oxidative stress, which can be detrimental particularly during the solventogenesis phase when the bacteria are already being exposed to gradually increasing solvent stress.

Conclusion

Based on our experimental results, it can be hypothesized that future microbial engineering studies on *Clostridium* strains should focus on methods to manage the stresses within the target organisms so as to improve butanol production on the one hand and riboflavin

production on the other. To our knowledge the present study is the first of its kind where an extensive proteome profiling was carried out for a solventogenic bacteria which can utilize both five and six carbon sugars; the data and findings of this study would attract scientists and metabolic engineers to design efficient solvent producing organisms.

References

Bankar SB, Survase SA, Ojamo H, Granström T. 2013. Biobutanol: The outlook of an academic and industrialist. RSC Advances 3(47):24734-24757.

Bramono SE, Lam YS, Ong SL, He J. 2011. A mesophilic Clostridium species that produces butanol from monosaccharides and hydrogen from polysaccharides. Bioresource Technology 102(20):9558-9563.

Caranto JD, Weitz A, Hendrich MP, Kurtz DM. 2014. The nitric oxide reductase mechanism of a flavo-diiron protein: Identification of active-site intermediates and products. Journal of the American Chemical Society 136(22):7981-7992.

Chee SG, Poh KC, Trong KP, Wright PC. 2007. Technical, experimental, and biological variations in isobaric tags for relative and absolute quantitation (iTRAQ). Journal of Proteome Research 6(2):821-827.

Cornelis P, Wei Q, Andrews SC, Vinckx T. 2011. Iron homeostasis and management of oxidative stress response in bacteria. Metallomics 3(6):540-549.

Crossley RA, Gaskin DJH, Holmes K, Mulholland F, Wells JM, Kelly DJ, van Vliet AHM, Walton NJ. 2007. Riboflavin Biosynthesis Is Associated with Assimilatory Ferric Reduction and Iron Acquisition by Campylobacter jejuni. Applied and Environmental Microbiology 73(24):7819-7825.

Darwin AJ. 2005. The phage-shock-protein response. Mol Microbiol 57(3):621-8.

Fomenko DE, Koc A, Agisheva N, Jacobsen M, Kaya A, Malinouski M, Rutherford JC, Siu K-L, Jin D-Y, Winge DR and others. 2011. Thiol peroxidases mediate specific genome-wide regulation of gene expression in response to hydrogen peroxide. Proceedings of the National Academy of Sciences 108(7):2729-2734.

Ghosh D, Li Z, Tan XF, Lim TK, Mao Y, Lin Q. 2013. ITRAQ based quantitative proteomics approach validated the role of calcyclin binding protein (CacyBP) in promoting colorectal cancer metastasis. Molecular and Cellular Proteomics 12(7):1865-1880.

Ghosh D, Yu H, Tan XF, Lim TK, Zubaidah RM, Tan HT, Chung MCM, Lin Q. 2011. Identification of key players for colorectal cancer metastasis by iTRAQ quantitative proteomics profiling of isogenic SW480 and SW620 cell lines. Journal of Proteome Research 10(10):4373-4387.

Grimmler C, Held C, Liebl W, Ehrenreich A. 2010. Transcriptional analysis of catabolite repression in Clostridium acetobutylicum growing on mixtures of d-glucose and d-xylose. Journal of Biotechnology 150(3):315-323.

Haus S, Jabbari S, Millat T, Janssen H, Fischer RJ, Bahl H, King JR, Wolkenhauer O. 2011. A systems biology approach to investigate the effect of pH-induced gene regulation on solvent production by Clostridium acetobutylicum in continuous culture. BMC Systems Biology 5.

He J, Ritalahti KM, Yang KU, Koenigsberg SS, Löffler FE. 2003. Detoxificabon of vinyl chloride to ethene coupled to growth of an anaerobic bacterium. Nature 424(6944):62-65.

Helmann JD. 2014. Specificity of Metal Sensing: Iron and Manganese Homeostasis in Bacillus subtilis. Journal of Biological Chemistry 289(41):28112-28120.

Hillmann F, Riebe O, Fischer R-J, Mot A, Caranto JD, Kurtz Jr DM, Bahl H. 2009. Reductive dioxygen scavenging by flavo-diiron proteins of Clostridium acetobutylicum. FEBS Letters 583(1):241-245.

Hoskisson PA, Rigali S. 2009. Chapter 1 Variation in Form and Function: The Helix-Turn-Helix Regulators of the GntR Superfamily. In: Allen IL, Sima S, Geoffrey MG, editors. Advances in Applied Microbiology: Academic Press. p 1-22.

Hou S, Jones SW, Choe LH, Papoutsakis ET, Lee KH. 2013. Workflow for quantitative proteomic analysis of Clostridium acetobutylicum ATCC 824 using iTRAQ tags. Methods 61(3):269-276.

Hu S, Zheng H, Gu Y, Zhao J, Zhang W, Yang Y, Wang S, Zhao G, Yang S, Jiang W. 2011. Comparative genomic and transcriptomic analysis revealed genetic characteristics related to solvent formation and xylose utilization in Clostridium acetobutylicum EA 2018. BMC Genomics 12.

Janssen H, Döring C, Ehrenreich A, Voigt B, Hecker M, Bahl H, Fischer RJ. 2010. A proteomic and transcriptional view of acidogenic and solventogenic steady-state cells of Clostridium acetobutylicum in a chemostat culture. Applied Microbiology and Biotechnology 87(6):2209-2226.

Jin L, Zhang H, Chen L, Yang C, Yang S, Jiang W, Gu Y. 2014. Combined overexpression of genes involved in pentose phosphate pathway enables enhanced d-xylose utilization by Clostridium acetobutylicum. Journal of Biotechnology 173(0):7-9.

Jones JA, Toparlak TD, Koffas MAG. 2015. Metabolic pathway balancing and its role in the production of biofuels and chemicals. Current Opinion in Biotechnology 33:52-59.

Kim S, Dale BE. 2015. Comparing alternative cellulosic biomass biorefining systems: Centralized versus distributed processing systems. Biomass and Bioenergy 74(0):135-147.

Lehninger AL, Nelson DL, Cox MM. 2008. Lehninger principles of biochemistry. New York: W.H. Freeman. xxix, 1158 p. p.

Li J, Huang C, Zheng D, Wang Y, Yuan Z. 2012. CcpA-mediated enhancement of sugar and amino acid metabolism in Lysinibacillus sphaericus by NMR-based metabolomics. Journal of Proteome Research 11(9):4654-4661.

Mishra B, Basu A, Chua RRY, Saravanan R, Tambyah PA, Ho B, Chang MW, Leong SSJ. 2014. Site specific immobilization of a potent antimicrobial peptide onto silicone catheters: evaluation against urinary tract infection pathogens. Journal of Materials Chemistry B 2(12):1706-1716.

Model P, Jovanovic G, Dworkin J. 1997. The Escherichia coli phage-shock-protein (psp) operon. Molecular Microbiology 24(2):255-261.

Oppenheimer-Shaanan Y, Wexselblatt E, Katzhendler J, Yavin E, Ben-Yehuda S. 2011. C-di-AMP reports DNA integrity during sporulation in Bacillus subtilis. EMBO Reports 12(6):594-601.

Peralta-Yahya PP, Zhang F, Del Cardayre SB, Keasling JD. 2012. Microbial engineering for the production of advanced biofuels. Nature 488(7411):320-328.

Phillips ZEV, Strauch MA. 2002. Bacillus subtilis sporulation and stationary phase gene expression. Cellular and Molecular Life Sciences 59(3):392-402.

Ren C, Gu Y, Hu S, Wu Y, Wang P, Yang Y, Yang C, Yang S, Jiang W. 2010. Identification and inactivation of pleiotropic regulator CcpA to eliminate glucose repression of xylose utilization in Clostridium acetobutylicum. Metabolic Engineering 12(5):446-454.

Ren C, Gu Y, Wu Y, Zhang W, Yang C, Yang S, Jiang W. 2012. Pleiotropic functions of catabolite control protein CcpA in Butanol-producing Clostridium acetobutylicum. BMC Genomics 13(1).

Riebe O, Fischer R-J, Bahl H. 2007. Desulfoferrodoxin of Clostridium acetobutylicum functions as a superoxide reductase. FEBS Letters 581(29):5605-5610.

Robertson JB, Gocht M, Marahiel MA, Zuber P. 1989. AbrB, a regulator of gene expression in Bacillus, interacts with the transcription initiation regions of a sporulation gene and

an antibiotic biosynthesis gene. Proceedings of the National Academy of Sciences 86(21):8457-8461.

Römling U. 2008. Great times for small molecules: C-di-AMP, a second messenger candidate in bacteria and archaea. Science Signaling 1(33).

Ross PL, Huang YN, Marchese JN, Williamson B, Parker K, Hattan S, Khainovski N, Pillai S, Dey S, Daniels S and others. 2004. Multiplexed protein quantitation in Saccharomyces cerevisiae using amine-reactive isobaric tagging reagents. Molecular and Cellular Proteomics 3(12):1154-1169.

Sadykov MR, Bayles KW. 2012. The control of death and lysis in staphylococcal biofilms: A coordination of physiological signals. Current Opinion in Microbiology 15(2):211-215.

Shala A, Patel KH, Golemi-Kotra D, Audette GF. 2013. Expression, purification, crystallization and preliminary X-ray analysis of the receiver domain of Staphylococcus aureus LytR protein. Acta Crystallographica Section F 69(12):1418-1421.

Sivagnanam K, Raghavan VGS, Shah M, Hettich RL, Verberkmoes NC, Lefsrud MG. 2011. Comparative shotgun proteomic analysis of Clostridium acetobutylicum from butanol fermentation using glucose and xylose. Proteome Science 9.

Szklarczyk D, Franceschini A, Kuhn M, Simonovic M, Roth A, Minguez P, Doerks T, Stark M, Muller J, Bork P and others. 2011. The STRING database in 2011: Functional interaction networks of proteins, globally integrated and scored. Nucleic Acids Research 39(SUPPL. 1):D561-D568.

Tracy BP, Gaida SM, Papoutsakis ET. 2008. Development and application of flow-cytometric techniques for analyzing and sorting endospore-forming clostridia. Applied and Environmental Microbiology 74(24):7497-7506.

Vasileva D, Janssen H, Honicke D, Ehrenreich A, Bahl H. 2012. Effect of iron limitation and fur gene inactivation on the transcriptional profile of the strict anaerobe Clostridium acetobutylicum. Microbiology 158(Pt 7):1918-29.

Vizcaíno Juan A, Csordas A, del-Toro N, Dianes JA, Griss J, Lavidas I, Mayer G, Perez-Riverol Y, Reisinger F, Ternent T and others. 2016. 2016 update of the PRIDE database and its related tools. Nucleic Acids Research 44(22).

Wang Q, Venkataramanan KP, Huang H, Papoutsakis ET, Wu CH. 2013. Transcription factors and genetic circuits orchestrating the complex, multilayered response of Clostridium acetobutylicum to butanol and butyrate stress. BMC Systems Biology 7.

Xin F, Wu YR, He J. 2014. Simultaneous fermentation of glucose and xylose to butanol by Clostridium sp. strain BOH3. Applied and Environmental Microbiology 80(15):4771-4778.

Ye X, Morgenroth E, Zhang X, Finneran KT. 2011. Anthrahydroquinone-2,6,-disulfonate (AH2QDS) increases hydrogen molar yield and xylose utilization in growing cultures of Clostridium beijerinckii. Appl Microbiol Biotechnol 92(4):855-64.

Ye X, Zhang X, Morgenroth E, Finneran KT. 2013. Exogenous anthrahydroquinone-2,6-disulfonate specifically increases xylose utilization during mixed sugar fermentation by Clostridium beijerinckii NCIMB 8052. International Journal of Hydrogen Energy 38(6):2719-2727.

Yeom J, Imlay JA, Park W. 2010. Iron homeostasis affects antibiotic-mediated cell death in Pseudomonas species. J Biol Chem 285(29):22689-95.

Zaldivar J, Nielsen J, Olsson L. 2001. Fuel ethanol production from lignocellulose: A challenge for metabolic engineering and process integration. Applied Microbiology and Biotechnology 56(1-2):17-34.

Zheng YN, Li LZ, Xian M, Ma YJ, Yang JM, Xu X, He DZ. 2009. Problems with the microbial production of butanol. Journal of Industrial Microbiology and Biotechnology 36(9):1127-1138.

Figure Legends

Figure 1. **(A)** iTRAQ workflow adopted for the proteomics study; **(B)** Physical significance of the iTRAQ ratios for the current study.

Figure 2. Production of butanol and riboflavin through anaerobic fermentation by strain BOH3 using glucose or xylose as the sole carbon source.

Figure 3. Flow-cytometric analysis of the xylose-fed **(A-D)** and glucose-fed **(E-H)** BOH3 cultures used for following proteomics studies.

Figure 4. (A) Proteins detected through the proteomics experiment which were classified using the cluster of orthologous gene (COG) classification method. C: Energy production and conversion; D: Cell division and Chromosome partitioning; E: Amino acid transport and metabolism; F: Nucleotide transport and metabolism; G: Carbohydrate Transport and Metabolism; H: Coenzyme metabolism; I: Lipid metabolism; J: Translation, ribosomal structure and biogenesis; K: Transcription; L: DNA replication, recombination and repair; M: Cell envelop biogenesis, outer membrane; N: Cell motility and secretion; O: protein turnover, chaperones (PTM); P: Inorganic ion transport and metabolism; Q: Secondary metabolites biosynthesis, transport and catabolism; R: General function prediction only; S: Function unknown; T: Signal transduction mechanisms; U: Intracellular trafficking and secretion; V: ABC transporter; X: Not in COG. **(B)** Classification of the regulated proteins corresponding to the acid phase (AP) , solvent phase (SP), Glucose dynamics (Gluc) and Xylose dynamics (Xyl). Refer to the text for definition of terms in (B). The scale provided indicates the number of proteins involved in each class.

Figure 5. Regulation profile of the COG-C regulated proteins corresponding to the AP1/2 and SP1/2 iTRAQ ratios. The proteins were manually clustered into groups C1 to C5 based

on the regulation profiles with details specified in the main text. (iTRAQ ratios of all the proteins used for generating the heat-map were converted to their log values with base 2.)

Figure 6. (A) Regulation profile of the selected important proteins within COG-H corresponding to AP1/2 and SP1/2 iTRAQ ratios. (iTRAQ ratios of all the proteins used for generating the heat-map were converted to their log values with base 2.) **(B)** CAC0590-0593 represent the proteins belonging to riboflavin metabolism; the corresponding positions of the involved proteins within the riboflavin biosynthesis pathway, as obtained from the KEGG database is shown in the right panel. **(C)** Effect of iron on the riboflavin titres obtained from BOH3 through xylose fermentation. The lower panel shows the bacterial growth, butanol and riboflavin titres achieved; while the upper panel shows pictures of the fermentation bottles used to grow BOH3 with the corresponding amount of iron in the media. The yellow color within the bottles is indicative of the produced riboflavin.

Figure 7. (A) Protein regulation profile of the selected important proteins belonging to COG-G corresponding to AP1/2 and SP1/2 iTRAQ ratios. (iTRAQ ratios of all the proteins used for generating the heat-map were converted to their log values with base 2.) Among the COG-G proteins, the regulation profiles of the two operons, *viz.* CAC1341-1349 and CAC2610-2613, involved in carbohydrate uptake and utilization. (B) The corresponding gene-maps is shown in panel **B.** The transcription factor CAC3037, also known as ccpA to repress the CAC1341-1349 operon, does not show any regulation in the glucose and xylose fed BOH3 cultures.

Figure 8. Overview of the xylose metabolism within the BOH3 cells.

Table I. Proteins within COG-C and COG-O clusters regulated during Glucose and Xylose dynamics

		iTRAQ ratio				
Protein	**COGID**	**Xyl-1**	**Xyl-2**	**Gluc-1**	**Gluc-2**	**Name**
Proteins related to energy metabolism						
CAC2450	COG2033C	6.3162*	4.5099*	1.3157	1.2915	Desulfoferrodoxin
CAP0162	COG1454C	4.3848*	4.3966*	1.6888*	2.2411*	Aldehyde-alcohol dehydrogenase
CAC2449	COG0426C	3.1578*	3.2056*	0.7589	0.8793	Flavo-diiron protein FprA2
CAC3597	COG1592C	2.7979*	2.4943*	2.4071*	1.9873*	Reverse rubrerythrin-2
CAC2459	COG0674C	2.7041*	2.5474*	1.0879	1.2098	2-oxoacid:ferredoxin oxidoreductase, alpha subunit
CAC2448	COG1251C	2.6109*	2.9479*	0.7778	0.9197	NADH-rubredoxin oxidoreductase
CAC2452	COG0426C	2.5966*	2.4751*	1.2481	0.9746	Flavodoxin
CAC3657	COG1012C	2.5308*	2.5855*	1.0766	1.1703	NADP-dependent glyceraldehyde-3-phosphate dehydrogenase
CAC0116	COG1151C	2.2218*	1.6314*	1.4402*	1.4045*	Carbone-monoxide dehydrogenase, beta chain
CAC1027	COG0426C	1.8587*	1.5348*	1.2085	1.3851*	Flavo-diiron protein FprA1
CAC0718	COG0778C	1.847*	1.6762*	1.1125	1.0501	Ortholog ycnD B.subtilis, nitroreductase
CAC0587	COG0716C	1.8032*	1.7335*	1.1097	0.8394	Flavodoxin
CAC2458	COG1013C	1.7337*	2.9674*	0.8953	0.94	2-oxoacid ferredoxin oxidoreductase, beta subunit
Proteins related to Protein processing						
CAC3714	COG0071O	3.7109*	3.357*	1.7763*	1.402*	18 kDa heat shock protein
CAC1052	COG0330O	2.5572*	2.3347*	1.2339	1.3698*	Membrane protease subunit, stomatin/prohibiting homolog
CAC0869	COG0492O	2.3312*	2.3184*	0.9598	1.1305	Thioredoxin reductase
CAC3189	COG0542O	2.2917*	2.1237*	1.2375	1.4648*	ATPases with chaperone activity clpC
CAC1549	COG0386O	1.7193*	2.1289*	1.533*	1.7138*	Glutathione peroxidase
CAC0959	COG0542O	1.4508*	1.3602*	1.2796	1.5039*	Chaperone protein ClpB
CAC3306	COG2077O	1.4347*	1.5611*	1.0476	1.186	Probable thiol peroxidase
CAC2703	COG0459O	1.4201*	1.3557*	1.3077	1.0727	60 kDa chaperonin
CAC0279	COG0760O	0.7235$^{\lrcorner}$	0.7088$^{\lrcorner}$	1.4848*	1.1928	Peptidil-prolyl cis-trans isomerase

*iTRAQ ratios indicating protein up-regulation; $^{\lrcorner}$iTRAQ ratios indicating protein down-regulation

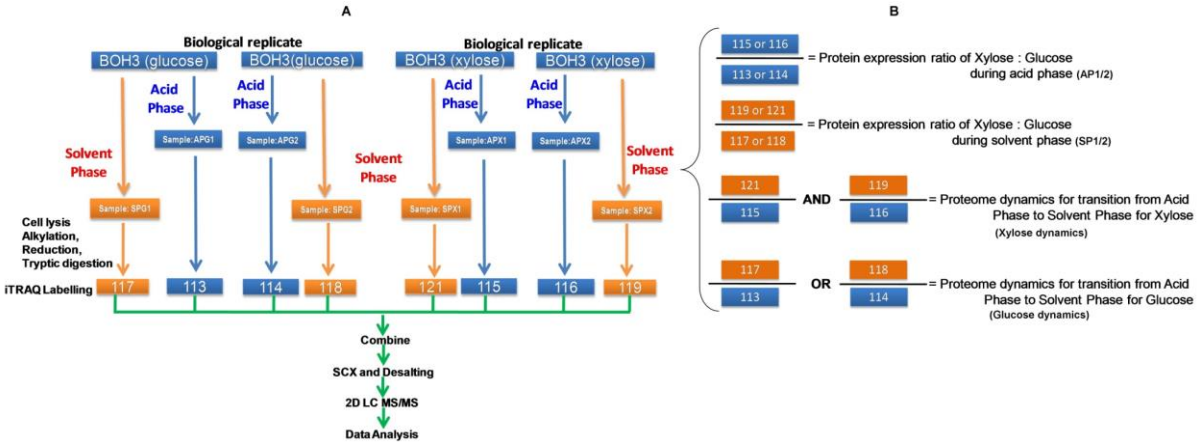

Figure 1

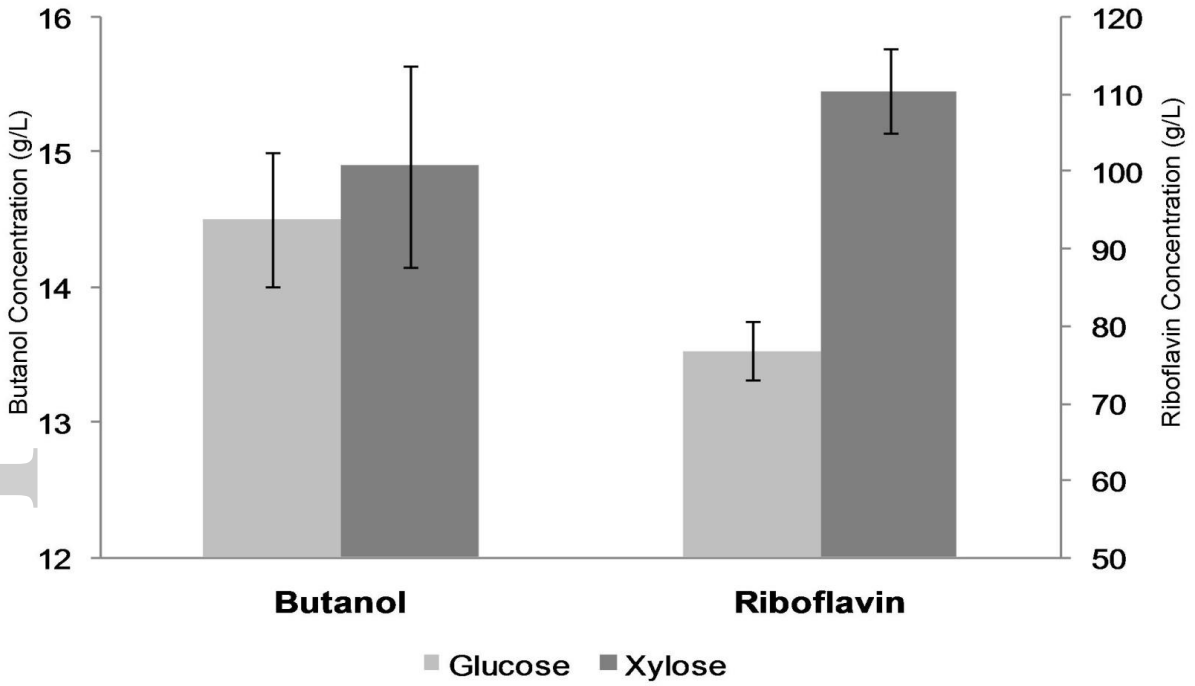

Figure 2

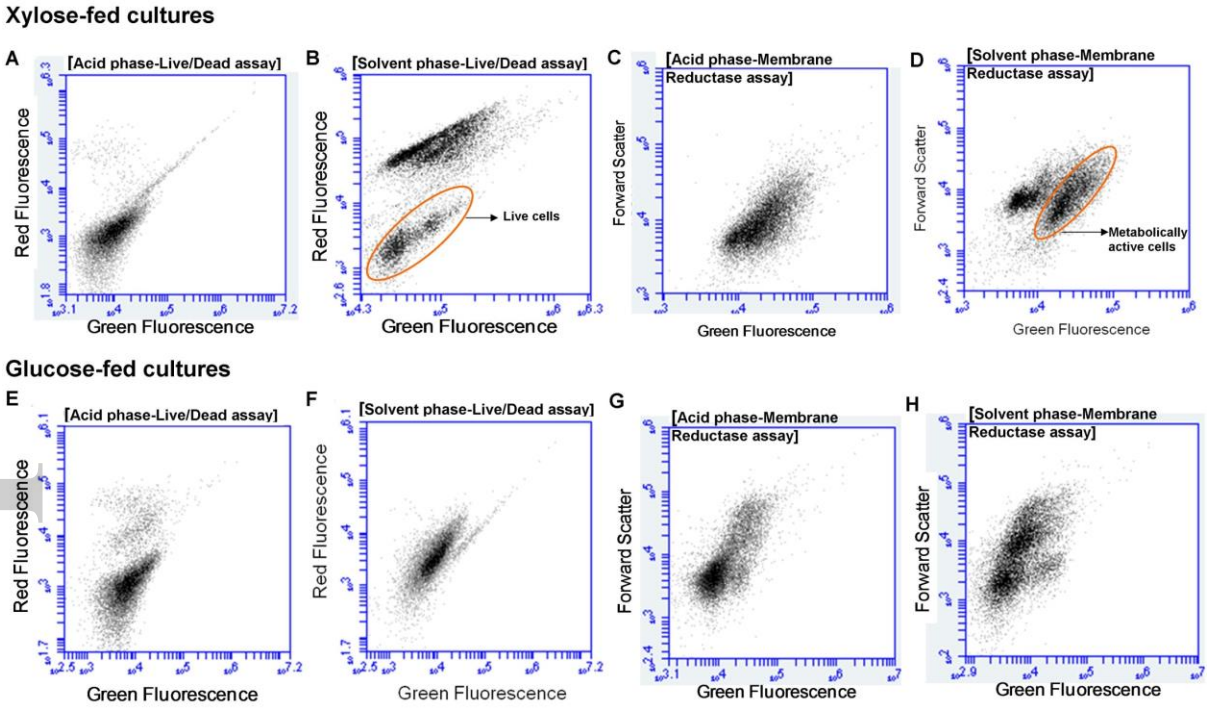

Figure 3

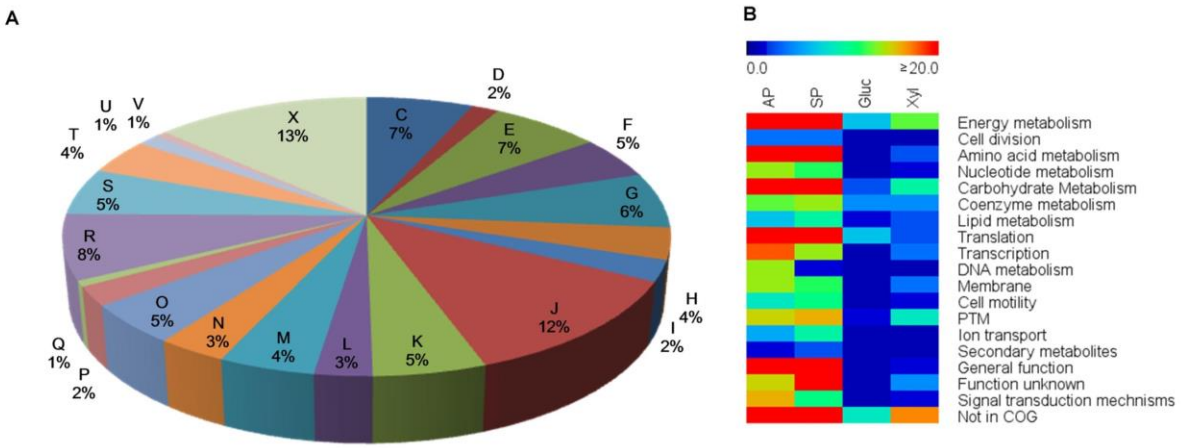

Figure 4

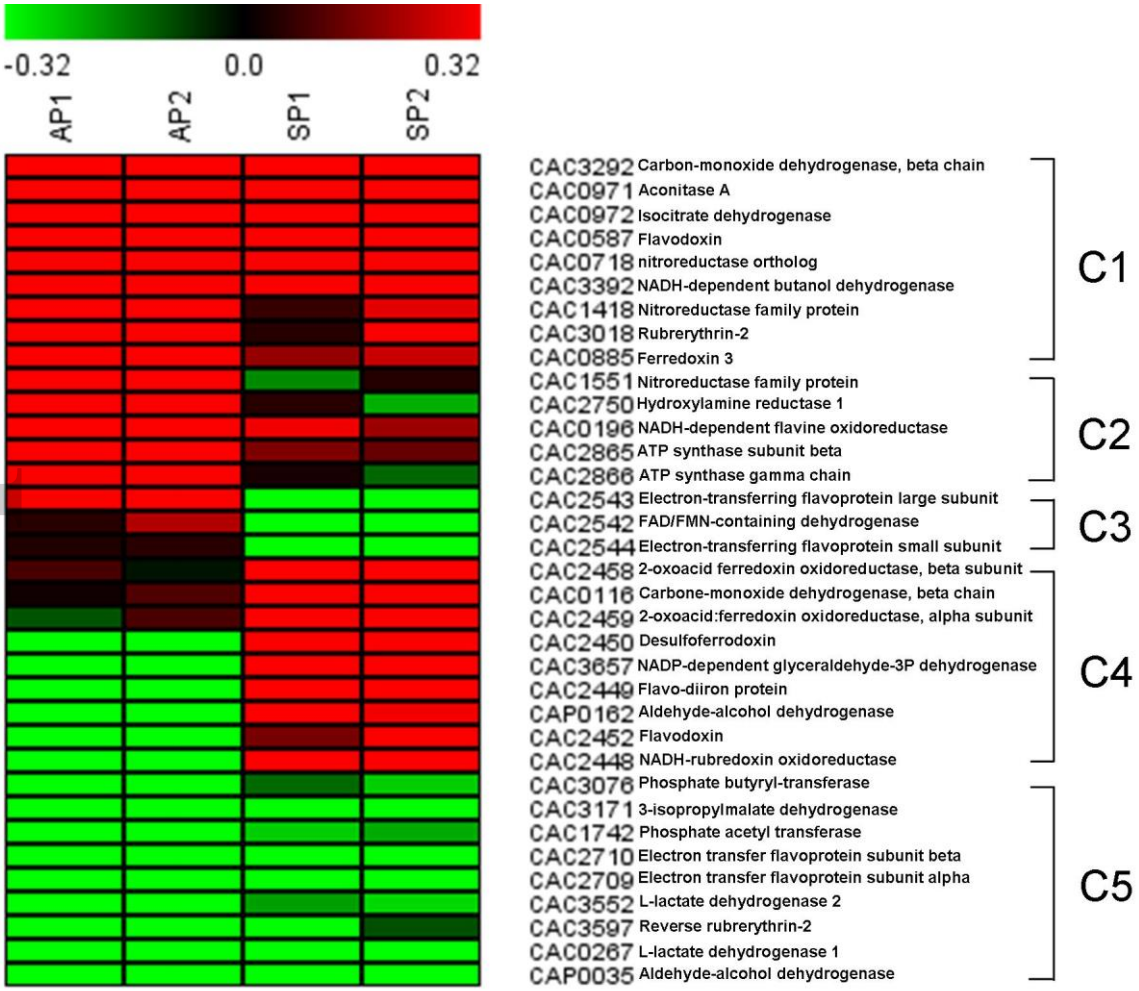

Figure 5

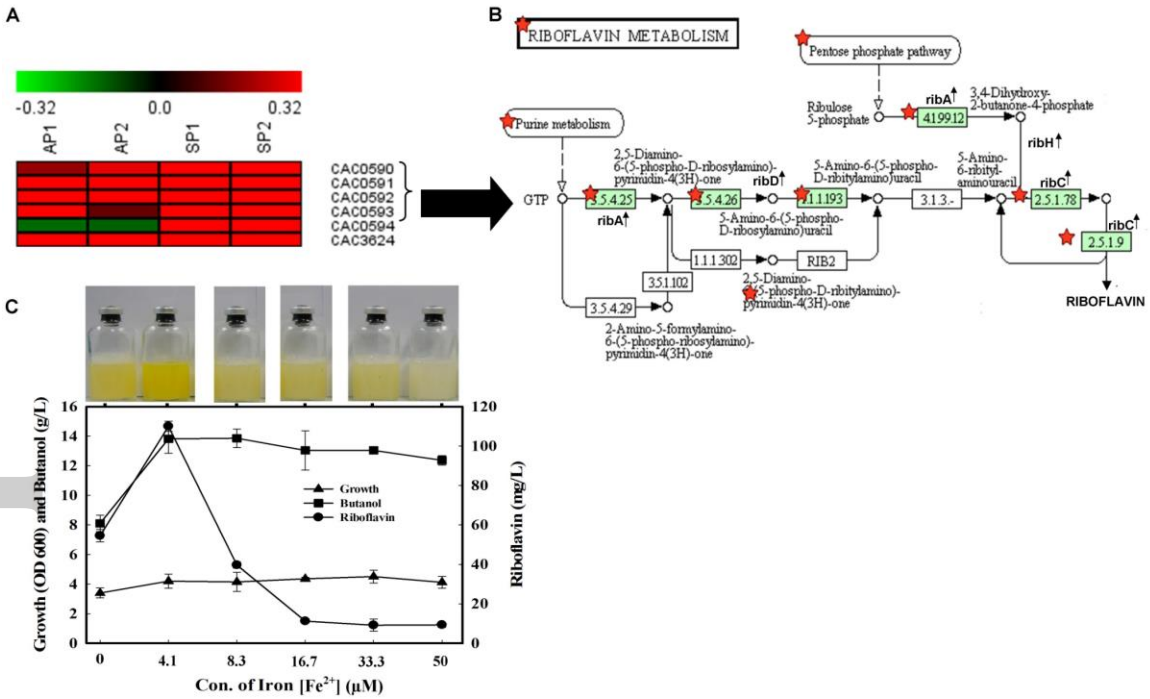

Figure 6

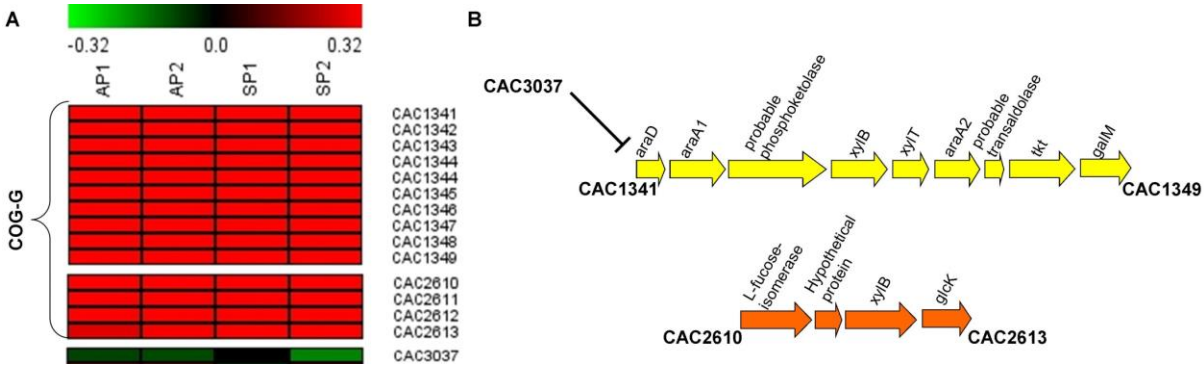

Figure 7

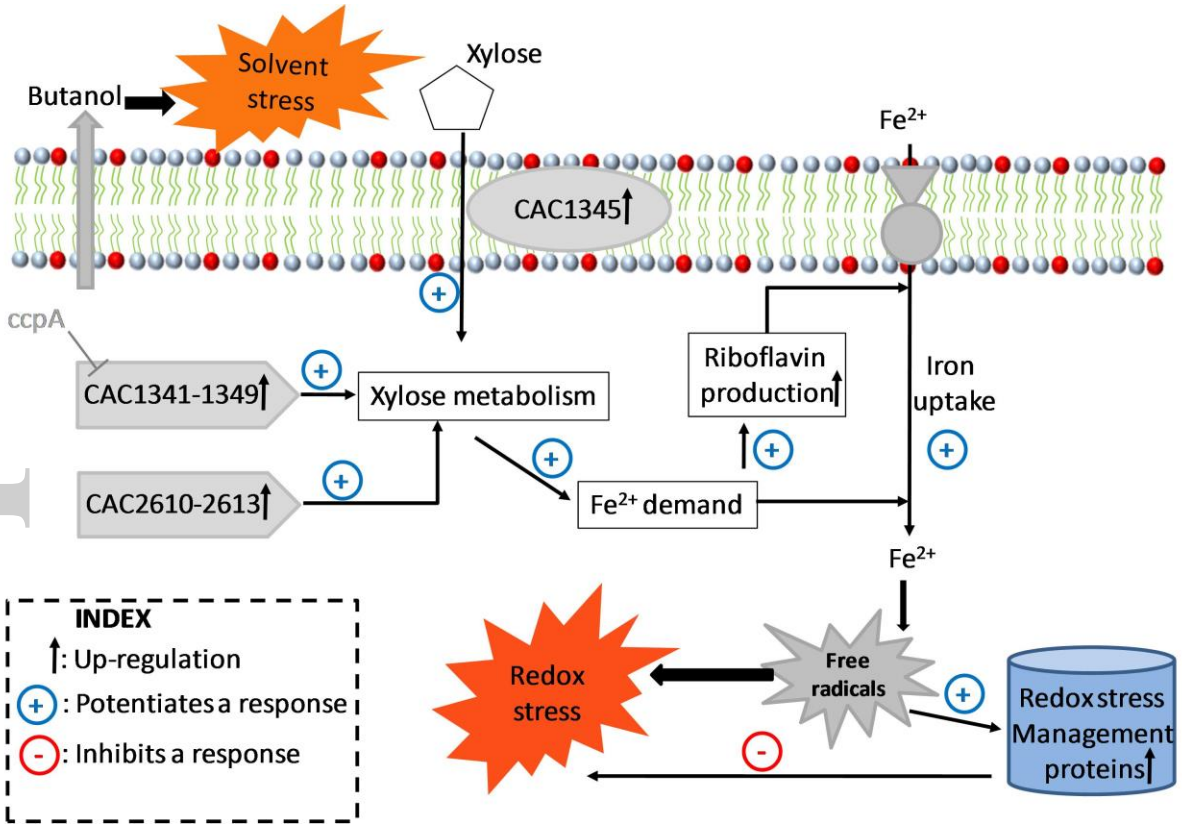

Figure 8